Bulletin of Faculty of Science, Zagazig University (BFSZU)
e-ISSN: 1110-1555
Volume-2024, Issue-1, pp-81-90
https://bfszu.journals.ekb.eg/journal
Research Paper DOI: 10.21608/bfszu.2023.229091.1297
==

Effect of an inclined load on a nonlocal fiber-reinforced visco-thermoelastic solid via a dual-phase-lag model

Samia M. Said [1*], Mohamed I.A. Othman [1], Esraa M. Gamal [1]

[1] Department of Mathematics, Faculty of Science, Zagazig University, P.O. Box 44519, Zagazig, Egypt.

Corresponding author: samia_said59@yahoo.com

***ABSTRACT:* In the present work, the effect of local and inclined loads on plane waves in a fiber-reinforced visco-thermoelastic solid will be investigated in the context of the dual-phase-lag model. The problem is solved numerically by the method of normal mode analysis. Numerical results for thermal temperature, displacement components, and stress are plotted and analyzed. Graphical results show that the effects of the angle of inclination and the nonlocal parameter are evident. Variations in these quantities are plotted in the context of the dual-phase-lag model with isolated boundaries to show the effects of nonlocal parameters and angle of inclination on wave propagation in the fiber-reinforced visco-thermoelastic solid. Compute the physical fields with suitable boundary conditions and perform numerical calculations using MATLAB programming. It was found that the inclined load plays a significant role in the distribution of all the physical quantities. The local parameter has a strong influence on the variation of all the physical quantities. The boundary conditions are met by all physical quantities.**
=

***KEYWORDS:* dual-phase lag-model, nonlocal parameter, fiber-reinforced, visco-thermoelastic,=inclined load.**

Date of Submission: 13-08-2023 Date of acceptance: 07-09-2023

I. INTRODUCTION

In 1972, Eringen (1972a) proposed the nonlocal continuum theory. The nonlocal elasticity theory, which provides meaning for small-scale effects, is established, along with the theory of nonlocal strain gradients, strain gradients, surface elasticity, and modified corresponding stress theories. Zenkour and Abouelregal (2016) discussed the influence of thermo-sensitive nanobeams using the thermoelasticity theory of the nonlocal solid with thermal relaxation time. Rotation's impact on a nonlocal, thermoelastic porous medium with a memory-dependent derivative was investigated by Said et al. (2022a). The nonlocal thermoelastic problem's analytical solutions were presented by Abbas et al. (2022). The nonlocal thermoelastic theory has been explained by many authors, such as Zhu et al. (2017), Sarkar et al. (2020a, 2020b), and Said et al. (2024).

The Kelvin-Voigt model is one of the most commonly used macroscopic models to describe the viscoelastic behaviour of materials. This model represents the delayed elastic response under load, where the deformation is time-varying but recoverable. Koltunov (1976) provided critical experimental results for determining the mechanical properties of viscoelastic materials. Said (2022) studied the effect of gravity on viscoelastic micro solids with voids and temperature. Gupta (2013) studied wave propagation in a viscoelastic transversely isotropic medium. Othman et al. (2002, 2017, 2018a), Said et al. (2022b), and Khoeini et al. (2023) discussed different kinds of thermo-viscoelastic problems.

Due to their exceptional qualities, fiber-reinforced polymers are utilized in many different industries. For the past few decades, fiber-reinforced materials' stress-deformation analysis has been a significant area of study in solid mechanics. In viscous, anisotropic, fiber-reinforced thermal media, Bayones and Hussien (2017) studied the propagation of Rayleigh waves under the impact of rotation. The effect of an inclined load on a functionally graded, temperature-dependent thermoelastic material was analyzed by Barak et al. (2022). Abbas and Othman (2011), Deswal et al. (2019), Abouelregal and Alesemi (2022), and Yadav et al. (2023) have studied many problems in fiber-reinforced thermoelastic materials.

The present problem discusses the effect of an inclined load and the nonlocal parameter on a fiber-reinforced visco-thermoelastic medium in the context of the dual-phase-lag model. The analytical solutions for the field variables of interest are obtained by using normal mode analysis to obtain the exact expressions for physical quantities. Numerical simulation results are obtained and plotted to show the effects of nonlocal parameters and an inclined load on wave propagation in a fiber-reinforced visco-thermoelastic medium. Results are compared with different values of the nonlocal parameter and with different values of the angle of inclination.

II. FORMULATION OF THE PROBLEM

We consider a nonlocal fiber-reinforced visco-thermoelastic anisotropic medium in a half-space $(x \geq 0)$. Plane strain in the $xy-$plane with the displacement vector $\boldsymbol{u} = (u, v, 0),\ \ u = u(x, y, t),\ \ v = v(x, y, t)$. Suppose that an inclined line load f_0 per unit length is acting on the z- axis and its inclination to x- axis is ϕ .

The constitutive equations are as in Belfield et al. (1983), Said (2020), and Eringen (1974).

$$(1-\varepsilon^2\nabla^2)\sigma_{ij} = \lambda^* e_{kk}\delta_{ij} + 2\mu_T{}^* e_{ij} + \alpha^*(a_k a_m e_{km}\delta_{ij} + a_i a_j e_{kk}) + 2(\mu_L{}^* - \mu_T{}^*)(a_i a_k e_{kj} + a_j a_k e_{ki}) - \gamma^*\theta\delta_{ij}$$
$$+\beta^* a_i a_j a_k a_m e_{km}, \tag{1}$$

The parameters $\lambda^*, \alpha^*, \mu_T{}^*, \mu_L{}^*, \beta^*$ and γ^* are defined as

$$\lambda^* = \lambda(1+\lambda_0\frac{\partial}{\partial t}),\ \ \alpha^* = \alpha(1+\alpha_0\frac{\partial}{\partial t}),\ \ \mu_T{}^* = \mu_T(1+\alpha_1\frac{\partial}{\partial t}),\ \ \mu_L{}^* = \mu_L(1+\alpha_2\frac{\partial}{\partial t}),\ \ \beta^* = \beta(1+\beta_0\frac{\partial}{\partial t}),$$
$$\gamma^* = \gamma(1+\gamma_0\frac{\partial}{\partial t}). \tag{2}$$

where, $\varepsilon = a_0 e_0$ is the elastic nonlocal parameter having a dimension of length, a_0, e_0 respectively, are an internal characteristic length and a material constant, σ_{ij} are the components of stress, e_{ij} are the components of strain, e_{kk} is the dilatation, λ, μ are elastic constants, [see Eringen et al. (1972b, 1972c) for details], $\alpha, \beta, (\mu_L - \mu_T)$ are reinforcement parameters, $\alpha_0, \alpha_1, \alpha_2, \beta_0, \gamma_0$ are the viscoelastic parameters, α_T is the thermal expansion coefficient, $\theta = T - T_0$ where T is the temperature above the reference temperature T_0, δ_{ij} is the Kronecker's delta, and $a \equiv (1,0,0)$ is fiber-direction $a \equiv (a_1, a_2, a_3),\ a_1{}^2 + a_2{}^2 + a_3{}^2 = 1$.

The equations of motion in the absence of body force

$$\sigma_{ji,j} = \rho\ddot{u}_i \tag{3}$$

The heat conduction equation in the context of dual-phase-lag model in the form

$$k^*(1+\tau_\theta\frac{\partial}{\partial t})\nabla^2 T = (1+\tau_q\frac{\partial}{\partial t})[\rho C_E\dot{T} + \gamma^* T_0\dot{e}). \tag{4}$$

Where k^* is the coefficient of thermal conductivity, C_E is the specific heat at constant strain, τ_θ is the phase-lag of the temperature gradient, τ_q is the phase-lag of heat flux, and ρ is the mass density.

Substituting (1) into (3), we get

$$(1-\varepsilon^2\nabla^2)\rho\frac{\partial^2 u}{\partial t^2} = A_1\frac{\partial^2 u}{\partial x^2} + A_2\frac{\partial^2 v}{\partial x\partial y} + A_3\frac{\partial^2 u}{\partial y^2} - \gamma(1+\gamma_0\frac{\partial}{\partial t})\frac{\partial\hat{T}}{\partial x}, \tag{5}$$

$$(1-\varepsilon^2\nabla^2)\rho\frac{\partial^2 v}{\partial t^2} = A_3\frac{\partial^2 v}{\partial x^2} + A_2\frac{\partial^2 u}{\partial x\partial y} + A_4\frac{\partial^2 v}{\partial y^2} - \gamma(1+\gamma_0\frac{\partial}{\partial t})\frac{\partial\hat{T}}{\partial y}, \tag{6}$$

where $A_1 = (\lambda^* - 2\mu_T{}^* + 4\mu_L{}^* + 2\alpha^* + \beta^*),\ \ A_2 = \lambda^* + \alpha^* + \mu_L{}^*,\ \ A_3 = \mu_L{}^*,\ \ A_4 = \lambda^* + 2\mu_T{}^*$.

Consider the following non-dimensional variables:

$$(x',y',\varepsilon',u',v')=\frac{1}{l_0}(x,y,\varepsilon,u,v),\ \ (t',\tau'_\theta,\tau'_q,\lambda'_0,\alpha'_0,\alpha'_1,\alpha'_2,\beta'_0,\gamma'_0)=\frac{c_0}{l_0}(t,\tau_\theta,\tau_q,\lambda_0,\alpha_0,\alpha_1,\alpha_2,\beta_0,\gamma_0),$$

$$\theta'=\frac{\gamma(T-T_0)}{\lambda+2\mu_T},\ \ \sigma'_{ij}=\frac{\sigma_{ij}}{\mu_T},\ \ l_0=\sqrt{\frac{k^*}{\rho C_E T_0}},\ \ c_0=\sqrt{\frac{\lambda+2\mu_T}{\rho}}. \tag{7}$$

Using the above non-dimensional variables defined in Eq. (7), the above governing equations take the following form:

$$(1-\varepsilon^2\nabla^2)\frac{\partial^2 u}{\partial t^2}=h_1\frac{\partial^2 u}{\partial x^2}+h_2\frac{\partial^2 v}{\partial x\partial y}+h_3\frac{\partial^2 u}{\partial y^2}-(1+\gamma_0\frac{\partial}{\partial t})\frac{\partial\theta}{\partial x}, \tag{8}$$

$$(1-\varepsilon^2\nabla^2)\frac{\partial^2 v}{\partial t^2}=h_3\frac{\partial^2 v}{\partial x^2}+h_2\frac{\partial^2 u}{\partial x\partial y}+h_4\frac{\partial^2 v}{\partial y^2}-(1+\gamma_0\frac{\partial}{\partial t})\frac{\partial\theta}{\partial y}, \tag{9}$$

$$(1+\tau_\theta\frac{\partial}{\partial t})\nabla^2\theta=(1+\tau_q\frac{\partial}{\partial t})\left[d_1\dot{\theta}+d_2(1+\gamma_0\frac{\partial}{\partial t})\dot{e}\right]. \tag{10}$$

Where $(h_1,h_2,h_3,h_4)=(\frac{A_1}{\rho c_0^{\,2}},\frac{A_2}{\rho c_0^{\,2}},\frac{A_3}{\rho c_0^{\,2}},\frac{A_4}{\rho c_0^{\,2}}),\ d_1=\frac{\rho C_E c_0 l_0}{k^*},\ d_2=\frac{\gamma^2 c_0 l_0 T_0}{k^*(\lambda+2\mu_T)}.$

III. NORMAL MODE ANALYSIS METHOD

We solve the problem of a nonlocal fiber-reinforced thermoelastic medium by using normal mode analysis as follows:

$$(u,v,\theta,\sigma_{ij})(x,y,t)=(\bar{u},\bar{v},\bar{\theta},\bar{\sigma}_{ij})(x)\,\mathrm{e}^{iby-mt}. \tag{11}$$

Where b is the wave number in the $y-$ direction, m is the complex constant, $\mathrm{i}=\sqrt{-1}$, and $\bar{u},\bar{v},\bar{\theta},\bar{\sigma}_{ij}$ are the amplitudes of the field quantities.

Using Eq. (11) in Eqs. (8)- (10), we get

$$(A_5\mathrm{D}^2-A_6)\bar{u}+(\mathrm{i}b\bar{h}_2\mathrm{D})\bar{v}-A_7\mathrm{D}\bar{\theta}=0, \tag{12}$$

$$(\mathrm{i}b\bar{h}_2\mathrm{D})\bar{u}+(A_8\mathrm{D}^2-A_9)\bar{v}-A_7\mathrm{i}b\bar{\theta}=0, \tag{13}$$

$$A_{10}\mathrm{D}\bar{u}+A_{11}\bar{v}+(A_{12}\mathrm{D}^2+A_{13})\bar{\theta}=0. \tag{14}$$

where $(\bar{h}_1,\bar{h}_2,\bar{h}_3,\bar{h}_4)=(\frac{\bar{A}_1}{\rho c_0^{\,2}},\frac{\bar{A}_2}{\rho c_0^{\,2}},\frac{\bar{A}_3}{\rho c_0^{\,2}},\frac{\bar{A}_4}{\rho c_0^{\,2}}),$

$$A_1=\lambda(1-\lambda_0 m)-2\mu_T(1-\alpha_1 m)+4\mu_L(1-\alpha_2 m)+2\alpha(1-\alpha_0 m)+\beta(1-\beta_0 m),$$

$$A_2=\lambda(1-\lambda_0 m)+\alpha(1-\alpha_0 m)+\mu_L(1-\alpha_2 m),\ \ A_3=\mu_L(1-\alpha_2 m),\ \ A_4=\lambda(1-\lambda_0 m)+2\mu_T(1-\alpha_1 m)$$

$$A_5=\bar{h}_1+m^2\varepsilon^2,\ \ A_6=m^2+b^2\bar{h}_3+m^2\varepsilon^2 b^2,\ \ A_7=(1-\gamma_0 m),\ A_8=\bar{h}_3+m^2\varepsilon^2,\ \ A_9=m^2+b^2\bar{h}_4+m^2\varepsilon^2 b^2,$$

$$A_{10}=d_2(1-\tau_q m)(1-\gamma_0 m),\ \ A_{11}=\mathrm{i}bA_{10},\ \ A_{12}=(1-\tau_\theta m),\ \ A_{13}=d_1 m(1-\tau_q m)-b^2(1-\tau_\theta m),$$

Eliminating $\bar{v}(x)$ and $\bar{\theta}(x)$ between Eqs. (12)- (14), we obtain the sixth-order ordinary differential equation satisfied with $\bar{u}(x)$

$$[\mathrm{D}^6-C_1\mathrm{D}^4+C_2\mathrm{D}^2-C_3]\bar{u}(x)=0. \tag{15}$$

$$C_1=\frac{(A_5A_9+A_6A_8)A_{12}-(A_7A_{10}+A_5A_{13})A_8-b^2\bar{h}_2^{\,2}A_{12}}{A_5A_8B_{12}},$$

$$C_2=\frac{A_6A_9A_{12}+b^2\bar{h}_2^{\,2}A_{13}+b^2\bar{h}_2A_7A_{10}+\mathrm{i}bA_5A_7A_{11}-A_7A_9A_{10}-(A_5A_9+A_6A_8)A_{13}-\mathrm{i}b\bar{h}_2A_7A_{11}}{A_5A_8A_{12}},$$

$$C_3=\frac{\mathrm{i}bA_6A_7A_{11}-A_6A_9B_{13}}{A_5A_8A_{12}}.$$

Equation (15) can be factorized as

$$(\mathrm{D}^2-k_1^{\,2})(\mathrm{D}^2-k_2^{\,2})(\mathrm{D}^2-k_3^{\,2})\bar{u}(x)=0 \tag{16}$$

Where $k_n^{\,2}\,(n=1,2,3)$ are the roots of the following characteristic equation

$$k^6 - C_1 k^4 + C_2 k^2 - C_3 = 0. \tag{17}$$

The solution of Eq. (15), which is bounded as $x \to \infty$, is given by

$$\bar{u}(x) = \sum_{i=1}^{3} N_i e^{-k_i x}, \tag{18}$$

$$\bar{v}(x) = \sum_{i=1}^{3} H_{1i} N_i e^{-k_i x}, \tag{19}$$

$$\bar{\theta}(x) = \sum_{i=1}^{3} H_{2i} N_i e^{-k_i x}, \tag{20}$$

Where $N_i (i = 1,2,3)$ are parameters. $H_{1i} = \dfrac{ib(A_6 + \bar{h}_2 k_i^2 - A_5 k_i^2)}{\bar{h}_2 k_i b^2 + A_8 k_i^3 - A_9 k_i}$, $H_{2i} = \dfrac{ib\bar{h}_2 k_i H_{1i} + A_6 - A_5 k_i^2}{A_7 k_i}$.

Substituting from Eq. (7) and (11) in Eq. (1), then using Eqs. (18) - (20), we obtain

$$\bar{\sigma}_{xx} = \sum_{i=1}^{3} H_{3i} N_i e^{-k_i x}, , \tag{21}$$

$$\bar{\sigma}_{yy} = \sum_{i=1}^{3} H_{4i} N_i e^{-k_i x}, \tag{22}$$

$$\bar{\sigma}_{xy} = \sum_{i=1}^{3} H_{5i} N_i e^{-k_i x}., \tag{23}$$

where $H_{3i} = \dfrac{-\bar{A}_1 k_i + ib\bar{B}_1 H_{1i} - (\lambda + 2\mu_T) A_7 H_{2i}}{[1-\varepsilon^2 (k_i^2 - b^2)]\mu_T}$, $H_{4i} = \dfrac{-k_i \bar{B}_1 + ib\bar{A}_4 H_{1i} - (\lambda + 2\mu_T) A_7 H_{2i}}{[1-\varepsilon^2 (k_i^2 - b^2)]\mu_T}$,

$H_{5i} = \dfrac{\bar{A}_3 (ib - k_i H_{1i})}{[1-\varepsilon^2 (k_i^2 - b^2)]\mu_T}$, and $\bar{B}_1 = \bar{A}_2 - \bar{A}_3$.

The normal mode analysis is, in fact, to look for the solution in the Fourier transformed domain, assuming that all the field quantities are sufficiently smooth on the real line such that normal mode analysis of these functions exists.

IV. THE BOUNDARY CONDITIONS OF THE PROBLEM

We consider an inclined load f_0 acting in the direction that makes an angle ϕ with the direction of $y-$axis as Othman et al. (2018b).

$$\frac{\partial\theta}{\partial x} = 0, \quad \sigma_{xx} = -F_1 e^{iby-mt} = -(f_0 \cos\phi) e^{iby-mt}, \quad \sigma_{xy} = -F_2 e^{iby-mt} = -(f_0 \sin\phi) e^{iby-mt}. \tag{24}$$

By inserting Eqs. (20)- (23) into Eq. (24), we have

$$\sum_{i=1}^{3} k_i H_{2i} N_i = 0, \quad \sum_{i=1}^{3} H_{3i} N_i = -f_0 \cos\phi, \quad \sum_{i=1}^{3} H_{5i} N_i = -f_0 \sin\phi. \tag{25}$$

Solving the above system of equations (25), we obtain a system of three equations. After applying the inverse matrix method, we have the values of the three constants. Hence, we obtain the expressions of displacements, temperature distribution, and the stress components:

$$\begin{pmatrix} N_1 \\ N_2 \\ N_3 \end{pmatrix} = \begin{pmatrix} k_1 H_{21} & k_2 H_{22} & k_3 H_{23} \\ H_{31} & H_{32} & H_{33} \\ H_{51} & H_{52} & H_{53} \end{pmatrix}^{-1} \begin{pmatrix} 0 \\ -f_0 \cos\phi \\ -f_0 \sin\phi \end{pmatrix}.$$

(26)

V. NUMERICAL RESULTS

We now show numerical findings for some physical constants to illustrate the theoretical conclusions obtained in the preceding section in the context of a dual-phase-lag model (DPL)

$\tau_\theta = 0.8$, $\tau_q = 0.9$, $\varepsilon = 0.99$, $f_0 = 0.9$, $\phi = 45$, $k^* = 386\,\mathrm{w.m^{-1}.K^{-1}}$, $T_0 = 293\,\mathrm{K}$, $C_E = 383.1\,\mathrm{J.kg^{-1}.K^{-1}}$,

$\lambda = 9.76 \times 10^9\ \mathrm{N.m^{-2}}$, $\beta = 2 \times 10^9\ \mathrm{N.m^{-2}}$, $\mu_T = 2.86 \times 10^{10}\ \mathrm{N.m^{-2}}$, $\mu_L = 3.45 \times 10^{10}\ \mathrm{N.m^{-2}}$, $\beta_0 = 1.96\,\mathrm{s^{-1}}$,

$\mu = 3.86\times10^{10}\ \mathrm{N.m^{-2}}$, $\alpha_T = 3.78\times10^{-4}\mathrm{K^{-1}}$, $\lambda_0 = 1.97\,\mathrm{s^{-1}}$, $\alpha_0 = 1.98\mathrm{s^{-1}}$, $\alpha_1 = 1.93\mathrm{s^{-1}}$, $\alpha_2 = 1.95\mathrm{s^{-1}}$, $\gamma_0 = 1.97\,\mathrm{s^{-1}}$, $\rho = 7800\,\mathrm{kg.m^{-3}}$, $m = m_0 + i\zeta$, $m_0 = -0.5$, $\zeta = 0.7$, $b = 0.38$, $y = -1.5$, $t = 0.2\mathrm{s}$.

Shown graphically in figures 1-4 are the displacement component v, the thermal temperature θ, and the stress components σ_{xx} and σ_{xy} in the case of three different values of the nonlocal parameter $(\varepsilon = 0.99,\ 0.7,\ 0)$ at $(\phi = 45^0)$. Figure 1 shows the distributions of the displacement component v in the case of $(\varepsilon = 0.99,\ 0.7,\ 0)$ and in the context of the DPL model. The displacement component v always begins from positive values and decreases in the range $0 \le x \le 6$, then converges to zero for $x \ge 6$. Figure 2 exhibits that the distribution of θ begins from positive values and decreases in the rang $0 \le x \le 6$ then converge to zero. It noticed that the distribution of θ decreases with the increase of the nonlocal parameter. Figures 3 and 4 show that the distribution of the stress components σ_{xx} and σ_{xy} begin from a negative value and satisfy the boundary conditions at $x = 0$. σ_{xx} and σ_{xy} increases in the range $0 \le x \le 6$, then converge to zero with increasing of the distance x at $x \ge 6$ in the context of the DPL model.

Figures 5-8 show the distribution of v, θ, σ_{xx} and σ_{xy} for three values of ϕ $(\phi = 95,\ 70,\ 45)$, in the context of the DPL model. Figure 5 shows that the displacement component v begins from positive values and decreases in the range $0 \le x \le 6$ for $(\phi = 95,\ 70,\ 45)$. Figure 6 shows the variation of the thermal temperature θ in the case of $(\phi = 95,\ 75,\ 45)$, θ decreases in the rang $0 \le x \le 6$, then converge to zero. Also, it observed that θ increases with the increase of ϕ. Figure 7 shows that σ_{xx} increases in the range $0 \le x \le 6$, then go to zero with increasing of the distance x at $x \ge 6$. It was noticed that the distribution of σ_{xx} decreases with the increase of ϕ. Figure 8 displays that the variations of the stress component σ_{xy} begin from a negative value and obey the boundary conditions in Eq. (23). It starts from negative value and reaches the maximum value in the range $0 \le x \le 6$, then converge to zero at $x \ge 6$.

Figures 9 and 10 display the 3D surface curves for the stress components within the framework of the DPL model. Different figures can be used to examine how different variables affect the vertical component of displacement. During wave propagation, all physical quantities are in motion; hence the vertical displacement has a significant impact on the curves that are produced.

VI. CONCLUION

The theoretical analysis and numerical calculations covered above enable us to reach the following important conclusions:

1) With an increase in distance *x*, all physical quantities' values go to zero.
2) The boundary conditions are met by all physical quantities.
3) The inclined load plays a significant role in the distribution of all the physical quantities.
4) Local parameter has a strong influence on the variation of physical quantities.
5) Analytical solutions based upon normal mode analysis for the thermoelastic problem in solids have been developed and utilized.

REFERENCES

1. Abbas, I. A., and Othman, M. I. A. Generalized thermoelastic interaction in a fiber-reinforced anisotropic half-space under hydrostatic initial stress. *J. Vib. Cont.* 18, 175–182 (2011).

2. Abbas, I.A., Hobiny A., Vlase S., and Marin, M. Generalized thermoelastic interaction in a half-space under a nonlocal thermoelastic model. *Mathematics.*10, 2168(2022).

3. Abouelregal, A. E., and Alesemi, M. Evaluation of the thermal and mechanical waves in anisotropic fiber-reinforced magnetic viscoelastic solid with temperature-dependent properties using the MGT thermoelastic model. *Case Stud. Therm. Eng.* 36, 102187(2022).

4. Bachher, M., and Sarkar, N. Nonlocal theory of thermoelastic materials with voids and fractional derivative heat transfer. *Wav. Ran. Comp.* 29, 595-613(2019).

5. Barak, M.S., and Dhankhar, P. Effect of inclined load on a functionally graded fiber-reinforced thermoelastic medium with temperature-dependent properties. *Acta Mech*. 233, 3645–3662(2022).

6. Bayones, F.S., and Hussien, N.S. Propagation of Rayleigh waves in fiber-reinforced anisotropic solid thermo-viscoelastic media under effect of rotation". *Appl. Math. Inf. Sci*. 11, 1527-1535(2017).

7. Belfield, A. J., Rogers, T. G., and Spencer, A. J. M. Stress in elastic plates reinforced by fiber lying in concentric circles. *J. Mech. Phys. Solid.* 31, 25–54(1983).

8. Deswal, S., Punia, B. S., and Kalkal, K. K. Reflection of plane waves at the initially stressed surface of a fiber-reinforced thermoelastic half space with temperature dependent properties. *Int. J. Mech. Mater. Des*. 15, 159–173(2019).

9. Eringen, A.C. Nonlocal polar elastic continua . *Int. J. Eng. Sci.* 10, 1–16 (1972a).

10. Eringen, A.C. Nonlocal polar elastic continua. *Int. J. Eng. Sci.*, 10(1), pp. 1–16(1972b).

11. Eringen, A.C., and Edelen D.G.B. On nonlocal elastic. *Int. J. Eng. Sci.* 10, 233–248(1972c).

12. Eringen, A.C. Theory of nonlocal thermoelasticity. *Int. J. Eng. Sci.*, 12, 1063-1077(1974).

13. Gupta, R. Reflection of waves in visco-thermoelastic transversely isotropic medium. Int. J. Comput. Meth. *Eng. Sci. Mech*. 14, 83-89(2013).

14. Khoeini, A., Imam A., and Najafi, M. Thermomechanical response of nonlinear viscoelastic materials. *J. Thermal Stress* 46, 588-605(2023).

15. Koltunov, M. Creeping and Relaxation. *Vysshaya Shkola, Moscow*(1976).

16. Othman, M.I.A., Magdy E., and El-Karamany, A. State space approach to two-dimensional generalized thermoviscoelasticity with one relaxation time. *J. Therm. Stress*. 25, 295-316(2002).

17. Othman, M.I.A., and Montaser, F. The Effect of Initial Stress on Generalized Thermo-viscoelastic Medium with Voids and Temperature-dependent Properties under Green-Naghdi Theory. *Mech. Mech. Eng.* 21, 291-308(2017).

18. Othman, M. I. A., and Montaser, F. Effect of rotation and gravity on generalized thermo-viscoelastic medium with voids. *Multi. Model. Mater. Struct*.14, 322-338(2018).

19. Othman, M. I. A., Abo-Dahab, S. M., and Alosaimi, H. A. The effect of gravity and inclined load in micropolar thermoelastic medium possessing cubic symmetry under G-N theory. *J. Ocean Eng. Sci.* 3, 288-294(2018).

20. Said, S.M. Novel model of thermo-magneto-viscoelastic medium with variable thermal conductivity under effect of gravity. *Appl. Math. Mech. Engl. Ed*. 41, 819–832(2020).

21. Said, S.M. A viscoelastic-micropolar solid with voids and micro-temperatures under the effect of the gravity field. *Geomech. Eng.* 31, 159-166(2022).

22. Said, S.M., Eldemerdash, M.G., and Othman, M.I.A. A novel model on nonlocal thermoelastic rotating porous medium with memory-dependent derivative. *Multi. Model. Mater. Struct.18*, 793-807(2022a).

23. Said, S.M., Abd-Elaziz, E.M., and Othman M.I.A. Effect of gravity and initial stress on a nonlocal thermo-viscoelasticmedium with two-temperature and fractional derivative heat transfer. *Z. Angew. Math. Mech*. 102, e202100316(2022b).

24. Said, S.M., Abd-Elaziz, E.M., and Othman, M.I.A. Wave propagation on a nonlocal porous medium with memory-dependent derivative and gravity. *Int. J. Comput. Mater. Sci. Eng.13*, 2350015(2024).

25. Sarker, N. Thermoelastic responses of a nonlocal elastic rod due to nonlocal heat conduction . *Z. Angew. Math. Mech.* 100, e201900252(2020a).

26. Sarkar, N., Mondal S., and Othman, M.I.A. Effect of the laser pulse on transient waves in a non-local thermoelastic medium under Green-Naghdi theory . *Struct. Eng. Mech.* 74, 471–479(2020b).

27. Yadav, K., Kalkal, K.K., and Sheoran, D. Thermodynamical interactions in a nonlocal initially stressed fiber-reinforced thermoelastic medium with microtemperatures under GN-II model. *J. Therm. Stress*. 46, 293-316(2023).

28. Zenkour, A.M., and Abouelregal, A.E. Nonlinear effects of thermo-sensitive nano- beams via a nonlocal thermoelasticity model with relaxation time . *Microsys. Techn.* 22, 2407–2415(2016).

29. Zhu, X.W., Wang, Y.B., and Dai, H.H. Buckling analysis of Euler–Bernoulli beams using Eringen two-phase nonlocal model . *Int. J. Eng. Sci*. 116, 130–140(2017).

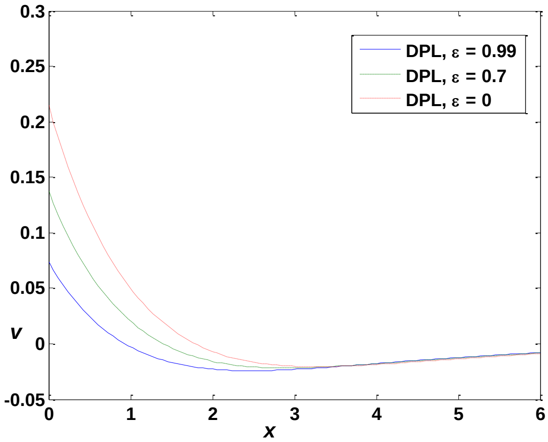

Figure 1 the displacement component v for different values of ε .

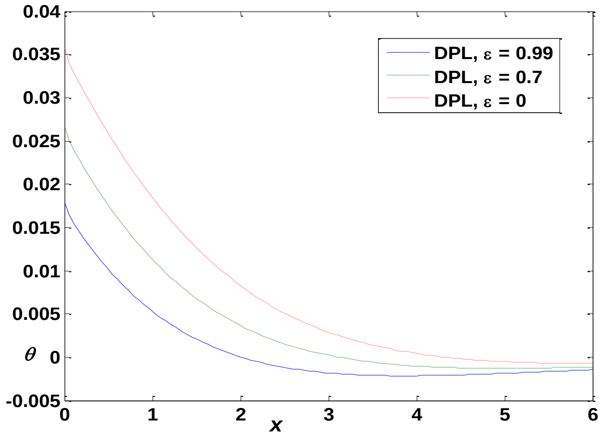

Figure 2 the thermal temperature component θ for different values of ε .

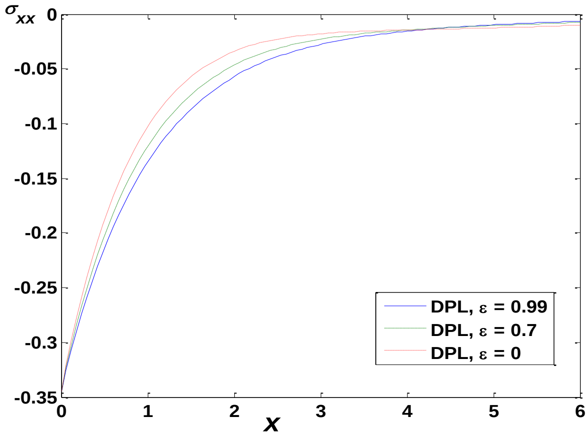

Figure 3 the stress component σ_{xx} for different values of ε .

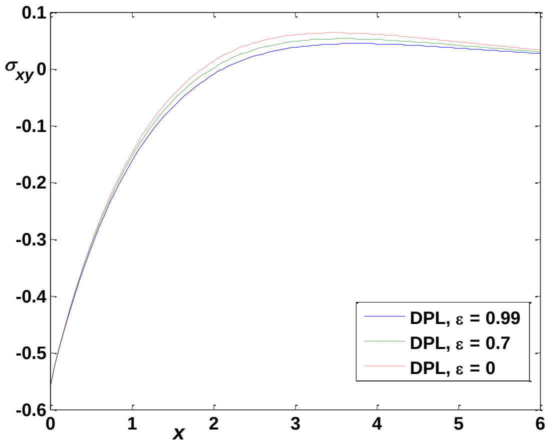

Figure 4 the stress component σ_{xy} for different values of ε .

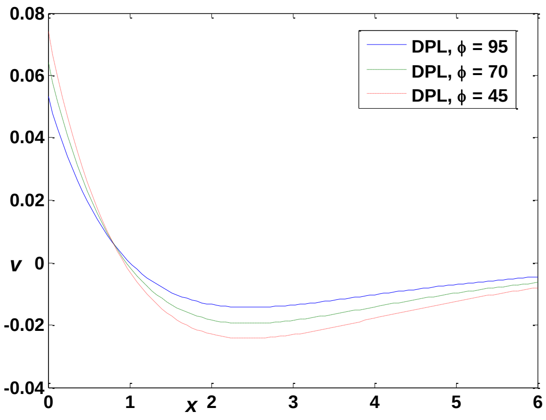

Figure 5 the displacement component v for different values of ϕ .

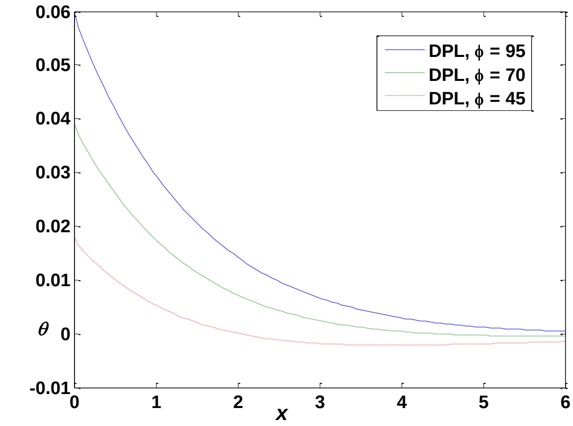

Figure 6 the thermal temperature component θ for different values of ϕ.

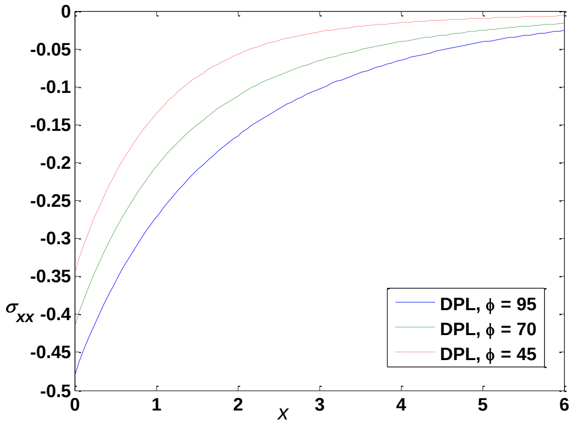

Figure 7 the stress component σ_{xx} for different values of ϕ.

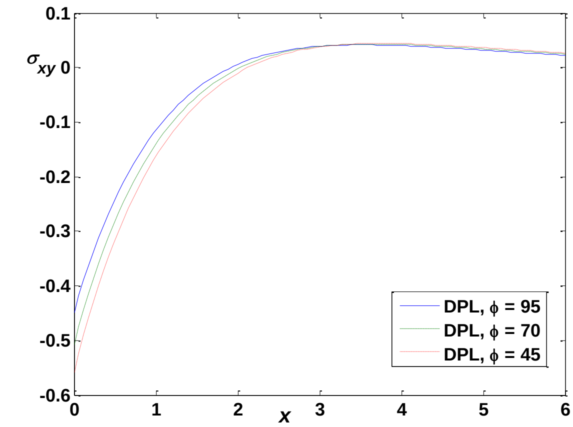

Figure 8 the stress component σ_{xy} for different values of ϕ.

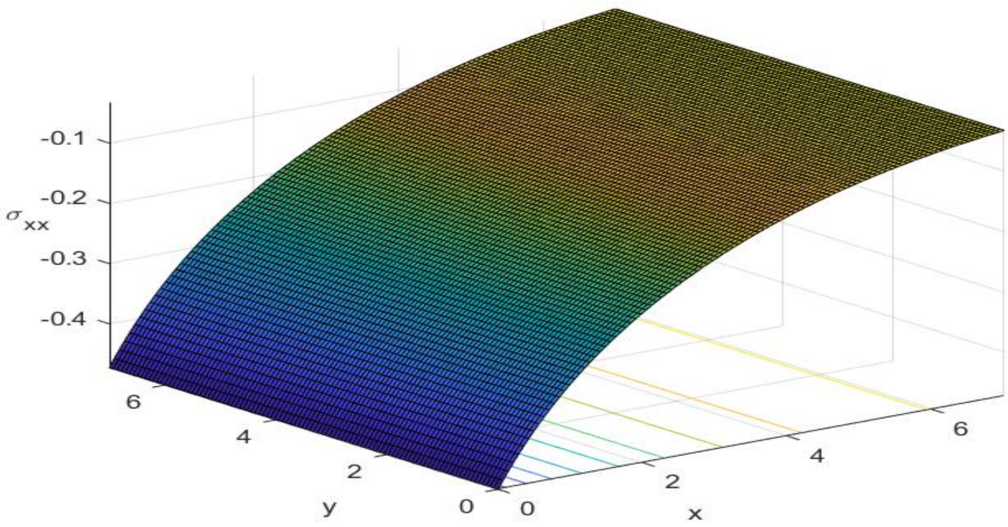

Figure 9 3D distribution of the stress component σ_{xx} in the context of DPL model

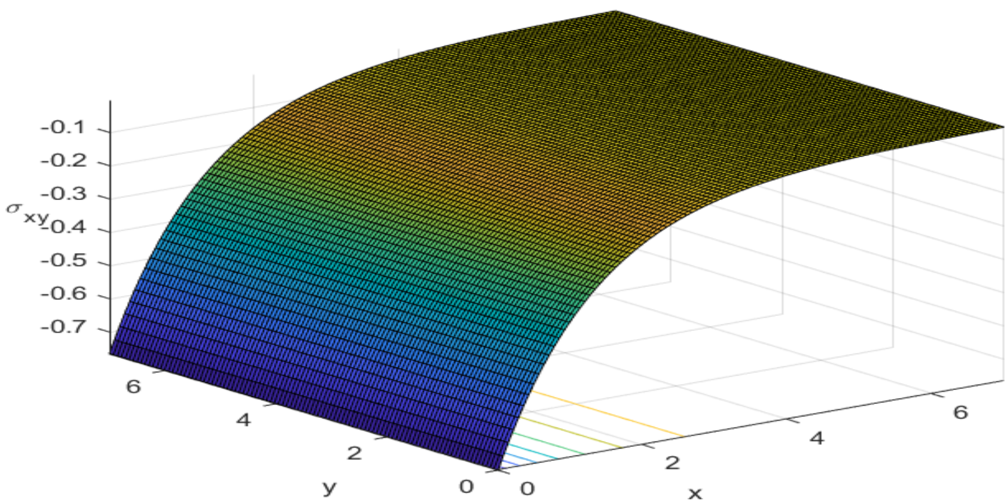

Figure 10 3D distribution of the stress component σ_{xy} in the context of DPL model